Article

Separation of Single-Walled Carbon Nanotubes on Silica Gel. Materials Morphology and Raman Excitation Wavelength Affect Data Interpretation

Christopher A. Dyke, Michael P. Stewart, and James M. Tour

J. Am. Chem. Soc., **2005**, 127 (12), 4497-4509• DOI: 10.1021/ja042828h • Publication Date (Web): 26 February 2005

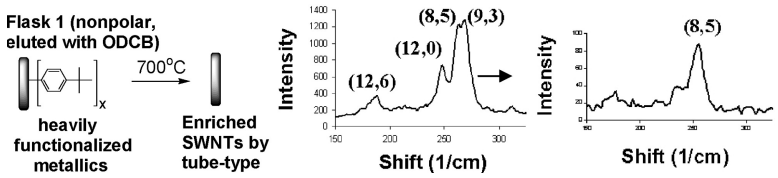

More About This Article

Additional resources and features associated with this article are available within the HTML version:

- Supporting Information
- Links to the 21 articles that cite this article, as of the time of this article download
- Access to high resolution figures
- Links to articles and content related to this article
- Copyright permission to reproduce figures and/or text from this article

View the Full Text HTML

J|A|C|S
ARTICLES
Published on Web 02/26/2005

Separation of Single-Walled Carbon Nanotubes on Silica Gel. Materials Morphology and Raman Excitation Wavelength Affect Data Interpretation

Christopher A. Dyke,† Michael P. Stewart,‡ and James M. Tour*

Contribution from the Departments of Chemistry and Mechanical Engineering and Materials Science, and Center for Nanoscale Science and Technology, Rice University, MS 222, 6100 Main Street, Houston, Texas 77005

Received November 29, 2004; E-mail: tour@rice.edu

Abstract: In this report, procedures are discussed for the enrichment of single-walled carbon nanotube (SWNT) types by simple filtration of the functionalized SWNTs through silica gel. This separation uses nanotube sidewall functionalization employing two different strategies. In the first approach, a crude mixture of metallic and semiconducting SWNTs was heavily functionalized with 4-*tert*-butylphenyl addends to impart solubility to the entire sample of SWNTs. Two major polarity fractions were rapidly filtered through silica gel, with the solvent being removed in vacuo, heated to 700 °C to remove the addends, and analyzed spectroscopically. The second approach uses two different aryldiazonium salts (one with a polar grafting group and one nonpolar), appended selectively onto the different SWNTs by means of titration and monitoring by UV analysis throughout the functionalization process. The different addends accentuate the polarity differences between the band-gap-based types permitting their partial separation on silica gel. Thermal treatment regenerated pristine SWNTs in enriched fractions. The processed samples were analyzed and characterized by Raman spectroscopy. A controlled functionalization method using 4-fluorophenyl and 4-iodophenyl addends was performed, and XPS analyses yielded data on the degree of functionalization needed to affect the van Hove singularities in the UV/vis/NIR spectra. Finally, we demonstrate that relative peak intensity changes in Raman spectra can be caused by morphological changes in SWNT bundling based on differing flocculation or deposition methods. Therefore a misleading impression of separations can result, underscoring the care needed in assessing efficacies in SWNT enrichment and the prerequisite use of multiple excitation wavelengths and similar flocculation or deposition methods in comparative analyses.

Introduction

Single-walled carbon nanotubes (SWNTs)[1] continue to inspire synthetic, theoretical, and technological interest. The fascination is due to important discoveries that are advancing fields such as optics, electronics, sensors, and composite materials science.[2] However, as with any new field, the rapid initial research pace without specific development of the analytical tools and protocols needed to make proper assessments can result in improper data interpretation. This is underscored here using a newly developed SWNT separation methodology as a case study. Although there is some level of enrichment of metallic SWNTs in the fractionated samples, the assignment of the enrichment levels could easily be inflated if not viewed with great care. As originally suggested by Strano and co-workers,[3] we describe here how morphological changes in SWNT deposition need to be scrutinized to properly assess the enrichment efficiencies using the commonly employed Raman spectroscopy for SWNT identification.

The diameter and vector in which a graphene sheet is conceptually rolled to form a nanotube is defined by two integers, n and m, which define the nanotube type. There are three cases for considering band structure from the n and m values. When $n - m = 0$, the SWNTs are metallic-like with a band gap of 0 eV and they are referred to as armchair nanotubes. When $|n - m| = 3q$, where q is a nonzero integer, the SWNTs are semimetallic-like, so-called "mod-3 tubes", with band gaps on the order of meV. All other nanotubes are semiconductors with a band gap varying between ca. 0.8−1.4 eV.[4] Herein, two broader nanotube categories will be referred to, namely metallics and semiconductors, where metallics includes both the meV band gap and 0 eV band gap structures.

All methods used to produce SWNTs generate a mixture of n,m types; therefore, a protocol to separate carbon nanotubes by type and/or sort nanotubes by a single structure is becoming increasingly desired for electronics and sensor applications. Thus

† Present address: Corporate Development Laboratory, NanoComposites, Inc., 8275 El Rio Street, Suite 130, Houston, TX 77054.

‡ Present address: Intel Research, SC1-19, 2200 Mission College Avenue, Santa Clara, CA 95054.

(1) Saito, R.; Dresselhaus, G.; Dresselhaus, M. S. *Physical Properties of Carbon Nanotubes*; Imperial College Press: London, 1998.
(2) (a) Ouyang, M.; Huang, J.-L.; Lieber, C. M. *Acc. Chem. Res.* **2002**, *35*, 1018. (b) Dai, H. *Acc. Chem. Res.* **2002**, *35*, 1035.
(3) Heller, D. A.; Barone, P. W.; Swanson, J. P.; Mayrhofer, R. M.; Strano, M. P. *J. Phys. Chem. B.* **2004**, *108*, 6905.
(4) O'Connell, M. J.; Bachilo, S. M.; Huffman, C. B.; Moore, V. C.; Strano, M. S.; Haroz, E. H.; Rialon, K. L.; Boul, P. J.; Noon, W. H.; Kittrell, C.; Ma, J.; Hauge, R. H.; Weisman, R. B.; Smalley, R. E. *Science* **2002**, *297*, 593.

Scheme 1. Separation Method I[a]

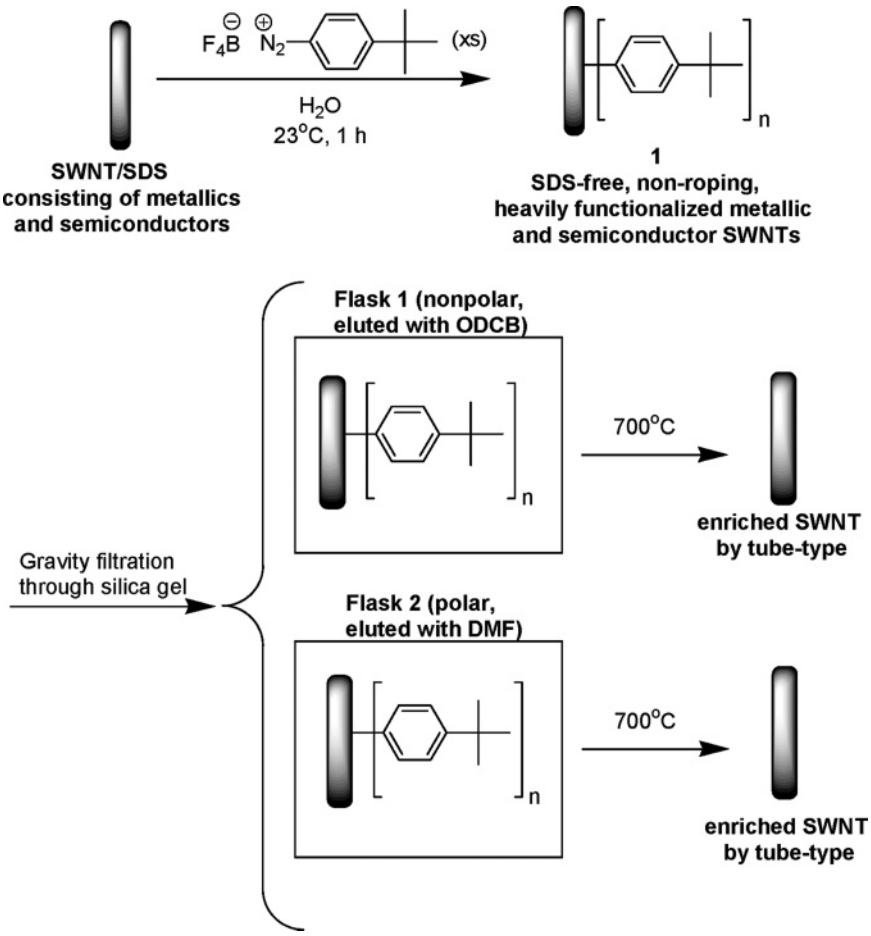

[a] Heavily functionalized SWNT are generated from SDS/SWNTs. The mixture of the functionalized metallic and semiconducting SWNTs is subject to filtration through silica gel generating a nonpolar band (eluted with *o*-dichlorobenzene) and a polar band (eluted with DMF). Thermolysis results in addend cleavage to generate enriched SWNT fractions by band gap.

several researchers have attempted to separate as-prepared material or to grow one particular nanotube type (possessing predominantly one *n*,*m* value).[5] There are several accounts of enrichment of nanotubes from a starting mixture, and they all take advantage of the electronic difference between the two carbon nanotube types, namely metallics vs semiconductors. Some of these reports use selective adsorption of the metallics with various chemical entities,[6−8] while others use electrophoresis[9] to separate by the differences in dipole moments induced by an electric field. We demonstrate here separations on HiPco-produced carbon nanotubes. The HiPco process affords samples containing ca. 50 different tube types (distinct *n*,*m* values), with ca. one-third of them having metallic character and two-thirds having semiconducting character.[4] Hence, our starting material is highly polydisperse in tube types, and therefore any utilization of this approach on less disperse starting samples will likely provide enhanced separations.

One must devise a method to maintain the SWNTs in unroped form for separations. SWNTs have a cohesive intertube attraction of 0.5 eV per nm of tube length and this must be overcome prior to their separation. We have previously shown that aryldiazonium salts can react with sodium dodecyl sulfate (SDS)-wrapped SWNTs (SWNT/SDS) in aqueous solutions to afford SWNT sidewall aryl addends with up to ca. 1 in 10 SWNT carbons being aryl-functionalized.[10] In the starting surfactant-wrapped form, the SWNTs remain dispersed as individuals rather than existing as bundled or roped structures (in this context we refer to bundles as ca. 2−5 SWNTs adhering to each other and ropes as >5 SWNTs adhering via their sidewalls). By slowly adding the aryldiazonium salts, the metallic SWNT sidewalls are preferentially functionalized, to the exclusion of the semiconductors' sidewalls.[10] Previously, however, we were unable to devise a simple separation scheme based upon this preferential reactivity.

Disclosed here are two different methods for the reaction/filtration/regeneration of enriched SWNT fractions: separation method I (Scheme 1) and separation method II (Scheme 2). In

(5) (a) Weisman, R. B. *Nat. Mater.* **2003**, *2*, 569. (b) Haddon, R. C.; Sippel, J.; Rinzler, A. G.; Papadimitrakopoulos, F. *Mater. Res. Soc. Bull.* **2004**, *29*, 253.
(6) Chen, Z. H.; Du, X.; Rancken, C. D.; Cheng, H. P.; Rinzler, A. G. *Nano Lett.* **2003**, *3*, 1245.
(7) Chattophadhyay, D.; Galeska, I.; Papadimitrakopoulos, F. *J. Am. Chem. Soc.* **2003**, *125*, 3370.
(8) Zheng, M.; Jagota, A.; Strano, M. S.; Santos, A. P.; Barone, P.; Chou, S. G.; Diner, B. A.; Dresselhaus, M. S.; McLean, R. S.; Onoa, G. B.; Samsonidze, G. G.; Semke, E. D.; Usrey, M.; Walls, D. J. *Science* **2003**, *302*, 1545.
(9) (a) Krupke, R.; Hennrich, F.; von Lohneysen, H.; Kappes, M. *Science* **2003**, *301*, 344. (b) Krupke, R.; Hennrich, F.; Kappes, M.; von Lohneysen, H. *Nano Lett.* **2004**, *4*, 1395. (c) Baik, S.; Usrey, M.; Rotkina, L.; Strano, M. S. *J. Phys. Chem. B* **2004**, *108*, 15560. (d) Heller, D. A.; Mayrhofer, R. M.; Baik, S.; Grinkova, Y. V.; Usrey, M. L.; Strano, M. S. *J. Am. Chem. Soc.* **2004**, *126*, 14567.
(10) Strano, M. S.; Dyke, C. A.; Usrey, M. L.; Barone, P. W.; Allen, M. J.; Shan, H. W.; Kittrell, C.; Hauge, R. H.; Tour, J. M.; Smalley, R. E. *Science* **2003**, *301*, 1519.

Scheme 2. Separation Method II[a]

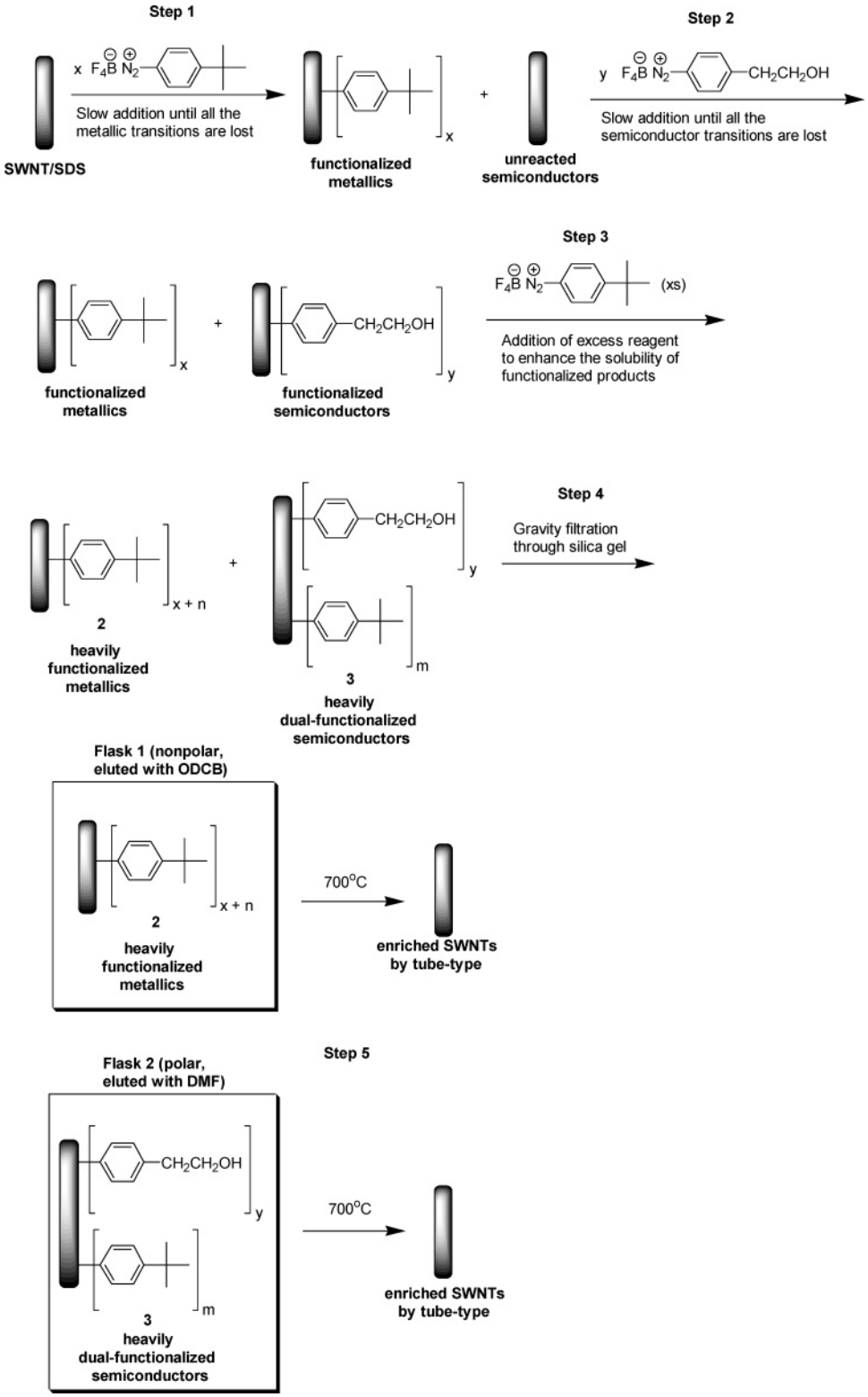

[a] Selective functionalization followed by completely functionalizing the SWNTs using two different polarity addends. The mixture of the functionalized metallic and semiconducting SWNTs is subject to filtration through silica gel generating a nonpolar band (eluted with *o*-dichlorobenzene) and a polar band (eluted with DMF). Thermolysis results in addend cleavage to generate enriched SWNT fractions by band gap.

separation method I, the mixture of SWNTs was heavily functionalized with 4-*tert*-butylphenyl addends to afford solubility to the entire mixture of SWNT types. Two major polarity fractions were separated by filtration through silica gel and then thermalized to remove the addends, followed by Raman analysis to discern enrichment of the SWNT types.

Separation method II is more complex, but it affords a complementary degree of purity for the metallic products. Once the *metallic* SWNTs had been preferentially reacted via titration with 4-*tert*-butylbenzenediazonium tetrafluoroborate (a nonpolar moiety) (Scheme 2, step 1), the *semiconducting* SWNTs were then titrated with a complementary aryldiazonium salt, 4-(2′-

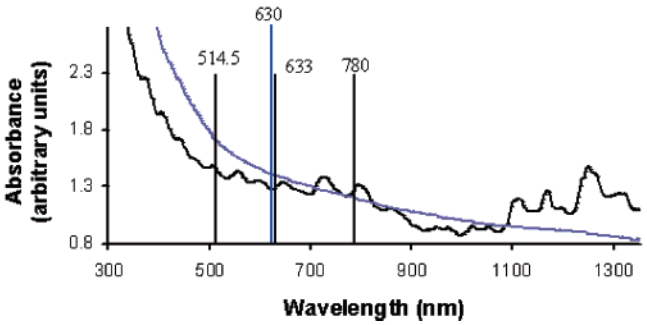

Figure 1. Absorption spectra of (a) SDS-coated SWNTs in water (black) and (b) SDS-coated SWNTs in water that have been heavily functionalized with 4-*tert*-butylbenzenediazonium tetrafluoroborate (blue) as described in separation method I (Scheme 1).

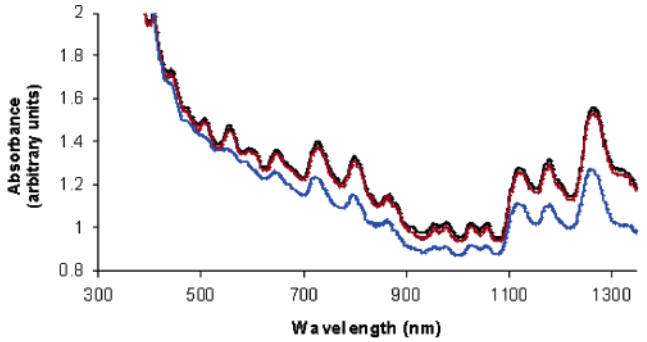

Figure 2. Absorption spectra of (a) starting SDS-coated SWNTs in water (black), (b) the same SDS-coated SWNTs after 15 additions of 4-*tert*-butylbenzenediazonium tetrafluoroborate (red), and (c) the same SDS-coated SWNTs after 24 additions of 4-*tert*-butylbenzenediazonium tetrafluoroborate (blue) as described in separation method II (Scheme 2).

hydroxyethyl)benzenediazonium tetrafluoroborate (a polar moiety) (Scheme 2, step 2), to serve as a different polarity-based SWNT sidewall addend. Both lightly functionalized SWNT types were then further functionalized with the non-polar addend (Scheme 2, step 3) to confer them with increased solubility and to prevent their rebundling or reroping upon removal of the SDS. This mixture was then subjected to a separation protocol using filtration through silica gel to generate enriched functionalized

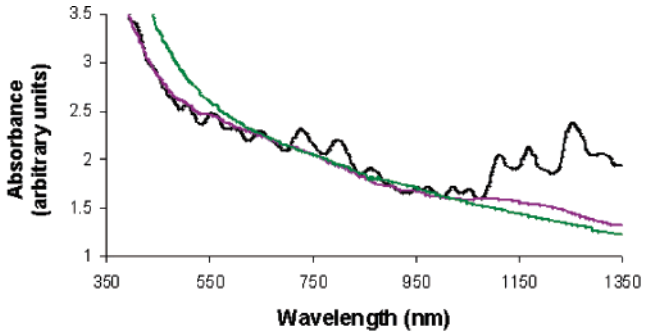

Figure 3. Absorption spectra of (a) starting material SDS/SWNTs (black), (b) after slow addition of the 4-fluorobenzenediazonium tetrafluoroborate until the transitions are lost (violet), and (c) after addition of an excess of the 4-iodobenzenediazonium tetrafluoroborate (blue) as described in Scheme 3.

metallic SWNTs (Scheme 2, step 4). Thermal treatment of the separated functionalized SWNTs removes the addends and regenerates two distinct fractions of the unfunctionalized SWNTs (Scheme 2, step 5), the first being enriched in metallic types.

When viewed in total, the separation methods described here afford some modest level of enrichment; however, less encouraging enrichment levels than would have been gleaned from comparative analyses based upon differing morphologies and singular Raman excitation wavelength studies. Therefore, the enrichment protocol here underscores the care needed in spectroscopically assessing SWNT purities.

Experimental and Analysis Section

Nanotube Synthesis and Individualized Materials Preparation. The raw, bulk nanotubes were prepared by the HiPco process[11] and obtained from the Carbon Nanotechnologies Laboratory, HiPco Center, at Rice University. This material, in general, has a diameter range from 0.6 to 1.3 nm with approximately 50 different SWNT types defined by *n* and *m*, containing metallics and semiconductors.[12,13] The iron catalyst used in the HiPco process gives an iron content of ca. 25 wt % with a small amount of amorphous carbon also present. The raw material was subjected to the published procedure[4,14,15] of surfactant wrapping to afford predominately individual SWNT/SDS in water with

Scheme 3. Iterative functionalization to determine coverage by TGA and XPS analysis.

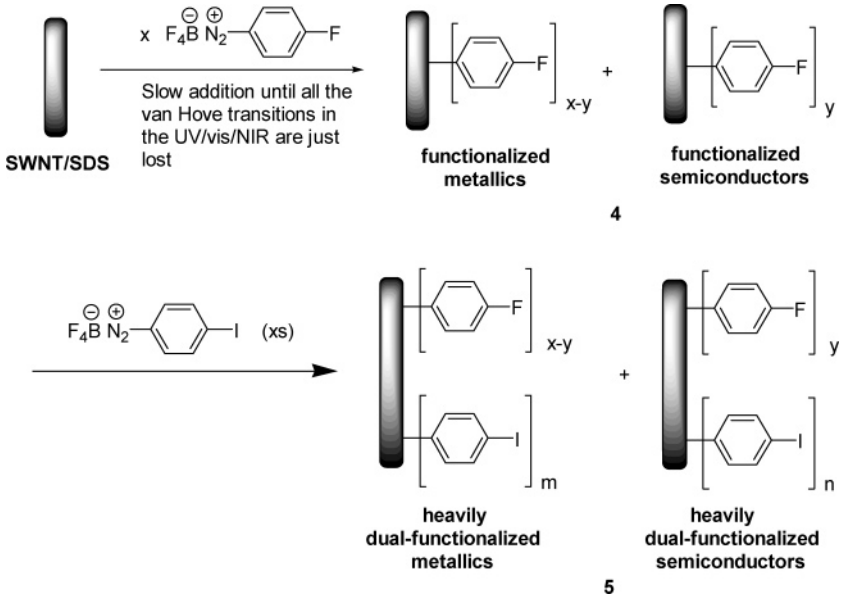

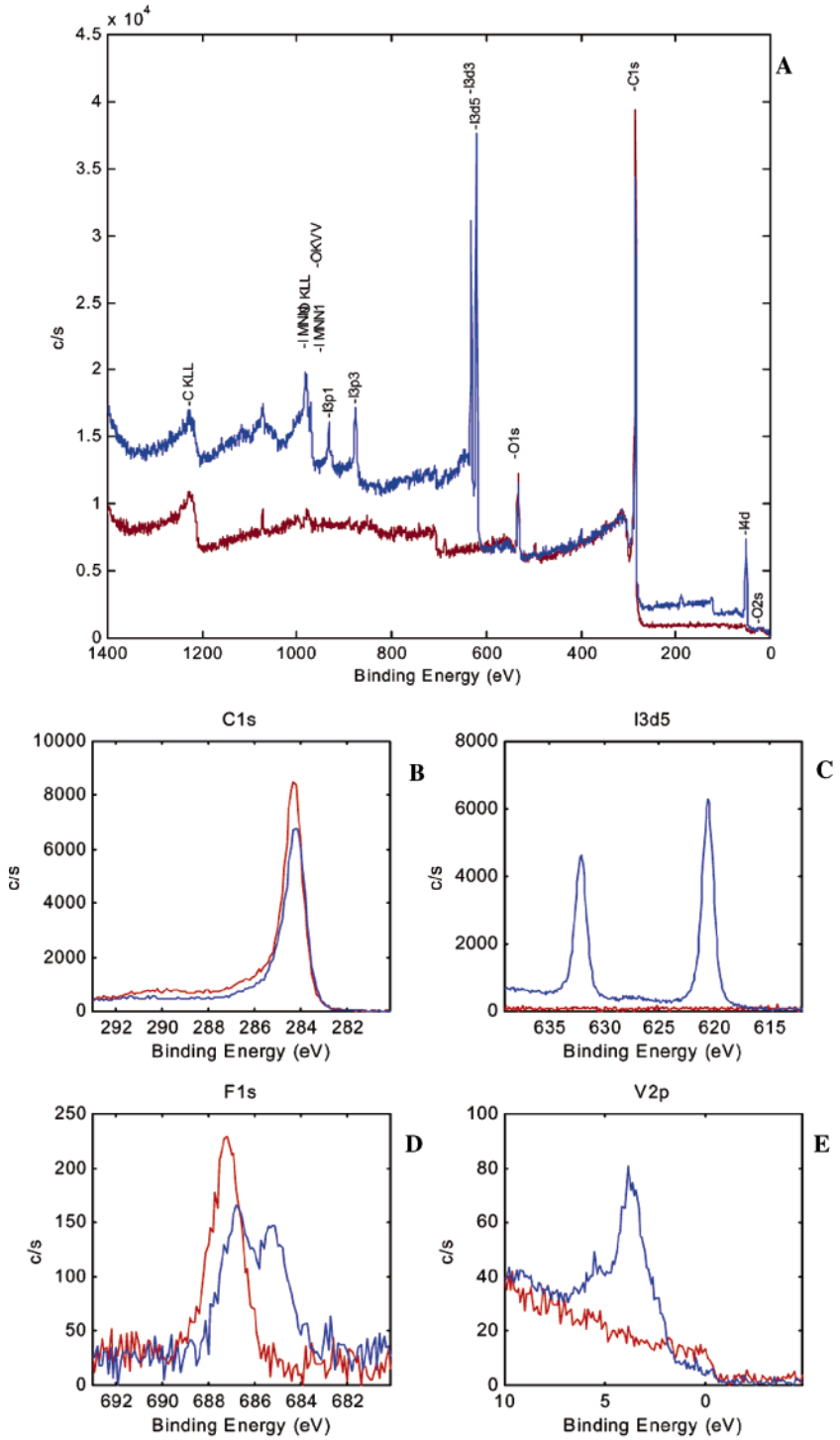

Figure 4. XPS analysis of the iterative functionalization products (aryl fluoride then aryl iodide as shown in Scheme 3), showing both the fluorinated material (red trace) and the fluoroaromatic-grafted material that was treated with 4-iodobenzenediazonium tetrafluoroborate (blue trace) after the van Hove transitions were lost in the UV/vis/NIR spectrum. XPS spectra were obtained at a 75° takeoff angle and 23.5 eV pass energy. The XPS analysis consisted of (A) survey of the spectral region from 0 to 1400 eV, (B) the carbon 1s region, (C) the iodine 3d5 region showing a strong presence of iodophenyl groups in the sample treated with 4-iodobenzenediazonium tetrafluoroborate, (D) the fluorine 1s region showing a slight decrease in the concentration and chemical state of the grafted fluorophenyl groups, and (E) the valence region showing a signal for iodine 5p at 3.5 eV only in the iodophenyl-grafted sample.

<2 wt % iron content. Specifically, the following protocol was used. The raw material (80 mg) is added to a flask loaded with SDS (2.0 g, 1 wt %). Ultrapure H_2O (200 mL) is then added to the vessel, and the aqueous solution is homogenized (Polyscience X-520, 750-Watt ultrasonic homogenizer) for 1 h. The freshly homogenized solution is sonicated in a cup-horn sonicator (Cole-Palmer CPX-600) for 10 min at 540 W. The sonicated mixture is centrifuged (Sorvall 100S Discovery Ultracentrifuge) at 30 000 rpm for 4 h. Centrifugation causes the more dense bundles and iron particles to sediment, and the upper 80 vol % portion is decanted to give predominately individual (nonbundled and nonroped) SWNT/SDSs while the lower 20 vol % contains SWNT ropes, SWNT bundles, and residual iron catalyst. Since the SWNTs now exist as SDS-wrapped individuals, the UV/vis/NIR spectra (Figure 1a) are not convoluted from bundling and clearly show transitions from both metallics (below 630 nm) and semiconductors (above 633 nm).[10] The concentration of the SWNTs varies from 20 to 25 mg/L of SDS-

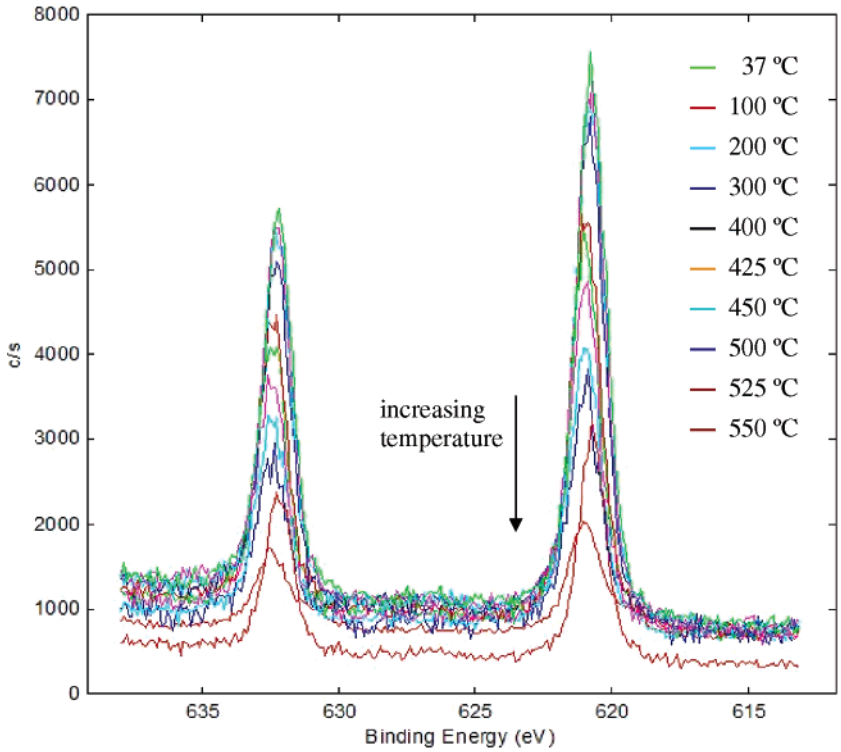

Figure 5. Iodine 3d region XPS of iodophenyl-functionalized SWNT material at 75° takeoff angle, undergoing heating from 37 °C to 550 °C at approximately 5 °C min^{-1} in UHV (5×10^{-9} Torr). At room temperature, the I $3d^{5/2}$ binding energy of 620.9 eV is consistent with an aryl iodide. At 550 °C, the same signal broadens and shifts to a lower binding energy of ca. 620.0 eV, indicating that the remaining iodine may exist as an inorganic salt.

coated SWNTs with greatly reduced iron content.[4,14,15] This material can be either heavily or selectively functionalized with diazonium salts depending on the procedure used, as discussed below.[10,16]

Separation Method I: Direct Heavily Functionalized SWNTs. Heavily functionalized material (Scheme 1) is obtained according to the published procedure[16] from the SWNT/SDS. The pH of the aqueous nanotube solution (100.0 mL, 0.002 mM, 0.20 meq of carbon) is adjusted to pH 10 with 1.0 M NaOH.[17] An excess of 4-*tert*-butylbenzenediazonium tetrafluoroborate (0.120 g, 0.48 mmol) is added as a solid to the SWNT/SDS solution. The reaction mixture is allowed to stir at rt for 1 h. The reaction is monitored by UV/vis/NIR to confirm loss of van Hove singularities (Figure 1b); complete loss of singularities is indicative of chemically functionalized sidewalls.[18,19] After this point, the solution is diluted with acetone which dissolves excess salt and causes the SDS to become dissociated from the SWNTs which immediately flocculate. The flocculated functionalized SWNTs are filtered over a PTFE-membrane (Sartorius, 0.45 μm pore size), and the solid functionalized nanotubes are collected and redispersed in DMF (10 mL) using a bath sonicator (Cole-Parmer Ultrasonic Cleaner 08849-00) for 1 min. The suspension is filtered a second time over a PTFE-membrane, washed with acetone, and the collected solid is then manipulated as needed (vide infra). The second filtration is performed to remove SDS and diazonium salt trapped during flocculation.

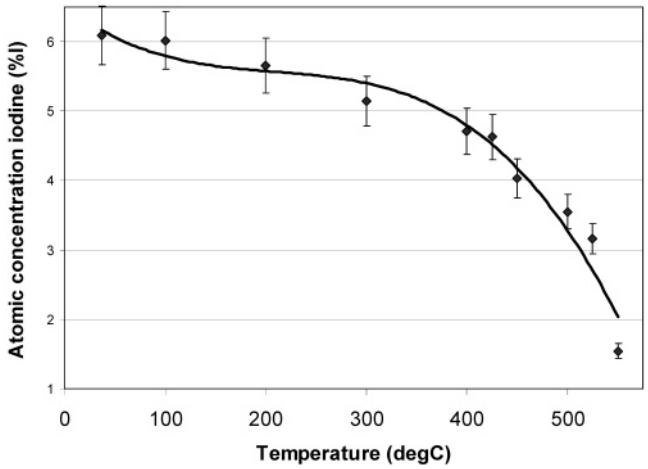

Figure 6. Atomic concentration iodine measured by XPS at 75° takeoff angle of iodophenyl-functionalized SWNT material. The thermal desorption of iodophenyl groups from carbon nanotube sidewalls shows a higher loss rate at temperatures above 425 °C, which is consistent with TGA measurements of similar material under inert gas (nitrogen) flow.[18,19]

The flocculated functionalized SWNTs are dispersed in *o*-dichlorobenzene (ODCB) (20 mL, 1 mL per 0.2 mg of functionalized SWNTs) by sonicating in a bath sonicator for 1 min. The solution was then introduced to a glass ODCB slurry-packed silica gel (silica gel, Davisil, grade 646, 35−60 mesh, Sigma-Aldrich) column. The column diameter was 2 in. with a 10-in. length of silica gel packing; this column loading required ca. 60 g of silica gel and 300 mL of ODCB to make the slurry. Use of finer grades of silica gel inhibits the functionalized SWNT elution. The chromatographic separation ensued by gravity using ODCB as the mobile (nonpolar) phase solvent. By simply visually monitoring the black-band progression, a faster moving band was noted and a second immobile band remained at the top of the column. Once the mobile band had fully eluted (ca. 50 mL of ODCB was used; 1 min from introduction of the functionalized nanotube solution), the solvent

(11) Nikolaev, P.; Bronikowski, M. J.; Bradley, R. K.; Rohmund, F.; Colbert, D. T.; Smith, K. A.; Smalley, R. E. *Chem. Phys. Lett.* **1999**, *313*, 91.
(12) Bachilo, S. M.; Strano, M. S.; Kittrell, C.; Hauge, R. H.; Smalley, R. E.; Weisman, R. B. *Science* **2002**, *5602*, 2361.
(13) Strano, M. S.; Doorn, S. K.; Haroz, E. H.; Kittrell, C.; Hauge, R. H.; Smalley, R. E. *Nano Lett.* **2003**, *3*, 1091.
(14) Strano, M. S.; Moore, V. C.; Miller, M. K.; Allen, M. J.; Haroz, E. H.; Kittrell, C.; Hauge, R. H.; Smalley, R. E. *J. Nanosci. Nanotech.* **2003**, *3*, 81.
(15) Moore, V. C.; Strano, M. S.; Haroz, E. H.; Hauge, R. H.; Smalley, R. E.; Schmidt, J.; Talmon, Y. *Nano Lett.* **2003**, *3*, 1379.
(16) Dyke, C. A.; Tour, J. M. *Nano Lett.* **2003**, *3*, 1215.
(17) Dyke, C. A.; Stewart, M. P.; Maya, F.; Tour, J. M. *Synlett* **2004**, 155.
(18) (a) Bahr, J. L.; Tour, J. M. *J. Mater. Chem.* **2002**, *12*, 1952. (b) Bahr, J.; Yang, J.; Kosynkin, D. V.; Bronikowski, M. J.; Smalley, R. E.; Tour, J. M. *J. Am. Chem. Soc.* **2001**, *123*, 6536.
(19) Dyke, C. A.; Tour, J. M. *Chem.—Eur. J.* **2004**, *10*, 813.

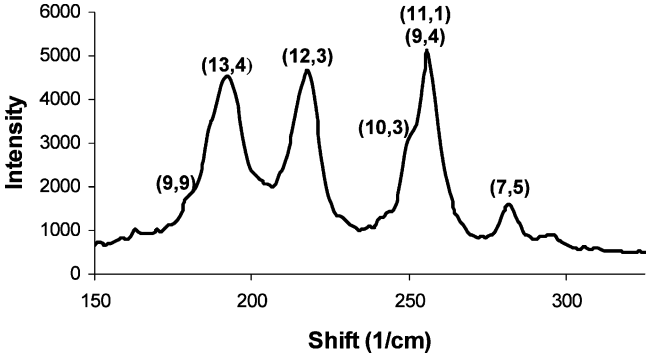

Figure 7. Raman (633 nm excitation) analysis of the starting SWNTs (prepared from the SDS/SWNTs by flocculation with acetone) radial breathing modes assigned to specific nanotubes.

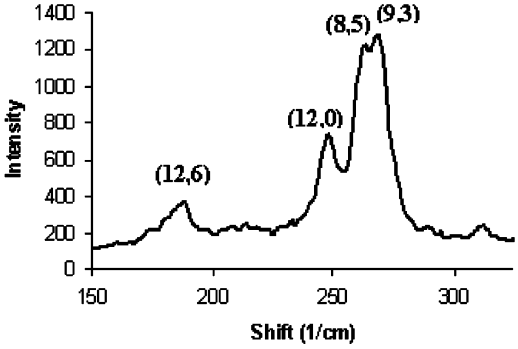

Figure 8. Raman (514.5 nm excitation) analysis of the starting SWNTs (prepared from the SDS/SWNTs by flocculation with acetone) radial breathing modes assigned to specific nanotubes.

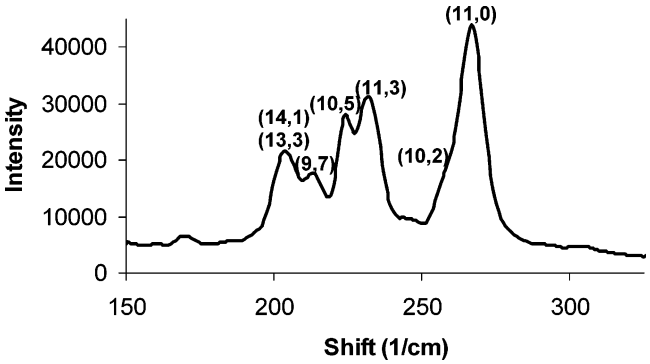

Figure 9. Raman (780 nm excitation) analysis of the starting SWNTs (prepared from the SDS/SWNTs by flocculation with acetone) radial breathing modes assigned to specific nanotubes.

was changed to DMF and the slower moving band (polar) eluted (ca. 250 mL of DMF was used) over a period of 15 min. This protocol separated the nanotubes into a nonpolar (faster-moving band) and a polar (slower-moving band) component. The two components were collected by filtering again over a PTFE membrane and evaporating to dryness. Of the 4.0 mg of functionalized material placed on the column, 3.2 mg were collected after gravity separation. The faster-moving component (nonpolar, flask 1 in Scheme 1) consisted of 1.3 mg of material, and the slower-moving (polar, flask 2 in Scheme 1) fraction had a weight of 1.9 mg. The functionalized material can be heated in an inert atmosphere (argon), and the addends evolve from the sidewalls of the SWNTs thereby regenerating the pristine, near-defect-free compounds in most cases; this was accomplished in a TGA apparatus. The loss of the addends begins at ca. 250 °C, and they are completely removed by 700 °C.[17,19] The regenerated, pristine nanotubes were analyzed by Raman spectroscopy to determine the content of nanotube types and AFM was used to determine length (vide infra).

Note that in addition to the silica gel described above, we also investigated other stationary phases. A large amount of the functionalized SWNTs was retained on the columns with stationary mesh sizes of 100 and above (the particles are 180 μm in diameter and smaller); however, silica gel (Sigma-Aldrich), polypyridine, or Dowex ion-exchange resins, 35−60 mesh, all allowed a substantial amount of the functionalized SWNTs to elute with little material trapped on the head of the column. Of the three stationary phases investigated, silica gel afforded the best enrichment by nanotube type.

Separation Method II: Selectively Functionalized SWNTs. SDS-coated SWNTs are selectively functionalized according to the published procedure.[10] The aqueous SWNT/SDS solution (150.0 mL, 0.002 mM, 0.31 mequiv of carbon) was divided into three portions each containing 50 mL, 0.002 mM, 0.10 mequiv of carbon so as to make the operation more manageable. To each of the three flasks, 4-*tert*-butylbenzenediazonium tetrafluoroborate (0.002 mM) is added in 10 μL portions to the starting SDS/SWNT solution every 30 min until the UV/vis transitions corresponding to the metallics (Figure 2a) are no longer present. After 24 additions to each flask, the selective functionalization (Scheme 2, step 1) is complete as indicated by the absorption spectrum (Figure 2c). A second solution, 4-(2-hydroxyethyl)benzenediazonium tetrafluoroborate (0.012 g, 0.05 mmol) in ultrapure H_2O (20 mL), is prepared. The 4-(2-hydroxyethyl)benzenediazonium tetrafluoroborate solution (0.003 mM) is added in 10 μL portions to each of the three SWNT/SDS solutions every 30 min (ca. 35 additions) until the UV/vis/NIR transitions corresponding to the semiconductors are no longer present (Scheme 2, step 2). An excess of the 4-*tert*-butylbenzenediazonium tetrafluoroborate (0.060 g, 0.40 mmol) is then added as a solid to each of the three SDS/SWNT solutions (Scheme 2, step 3). This excess appendage of 4-*tert*-butylphenyl moieties to all of the SWNTs prevents subsequent bundling and increases the solubility of the functionalized SWNTs in organic solvent[16,19,20] (ca. 0.7 to 0.5 mg/mL solubility in DMF and ODCB, respectively). The three solution flasks were combined into one and further worked up, filtered, and washed as described above.

The flocculated material from the selective functionalization reaction was dispersed in ODCB (20 mL total, 1 mL per 0.2 mg of functionalized SWNTs) by sonicating in a bath sonicator for 1 min. The functionalized SWNT mixture (4.0 mg) (**2** + **3**) was introduced onto an ODCB slurry-packed silica gel (silica gel, Davisil, grade 646, 35−60 mesh, Sigma-Aldrich) column packed as described above. Phases were separated by gravity first using ODCB as the mobile phase. Once the nonpolar component was collected in flask 1 (Scheme 2) which required ca. 50 mL of ODCB for the 1-min elution, the mobile phase was changed to DMF and the polar component fully eluted into flask 2 (Scheme 2) after using ca. 350 mL of DMF for 20 min. The materials in the separate flasks were filtered over a PTFE membrane. A total of 1.0 mg was lost on the head of the column, and of the remaining 3.0 mg of material collected, the faster-eluting band (nonpolar band) weighed 0.6 mg and the remainder of the weight (2.4 mg) corresponded to the slower-eluting band (polar component). Thermal treatment (Scheme 2, step 5), as described above, afforded the enriched SWNT samples.

Degree of Functional Group Coverage: UV−vis Transitions Correlated to XPS. XPS data were acquired on a Physical Electronics (PHI 5700) XPS/ESCA system with a typical base pressure of 5×10^{-9} Torr. A monochromatic Al X-ray source at 350 W was used with an analytical spot size of 1.2 mm and a 75° takeoff angle. Atomic concentration values were calculated with PHI Multipak software using factory calibrated values for the sensitivity factors of the respective elements (C 1s, O 1s, F 1s, I 3d). Binding energy values were referenced externally to an Au 4f peak at 84.00 eV and internally to a C 1s binding energy of 284.50 eV (NIST XPS database). Samples of functionalized SWNTs were flocculated from solution using acetone and filtered onto aluminum oxide membranes with a 100 nm average pore size (Whatman

(20) Dyke, C. A.; Tour, J. M. *J. Am. Chem. Soc.* **2003**, *125*, 1156.

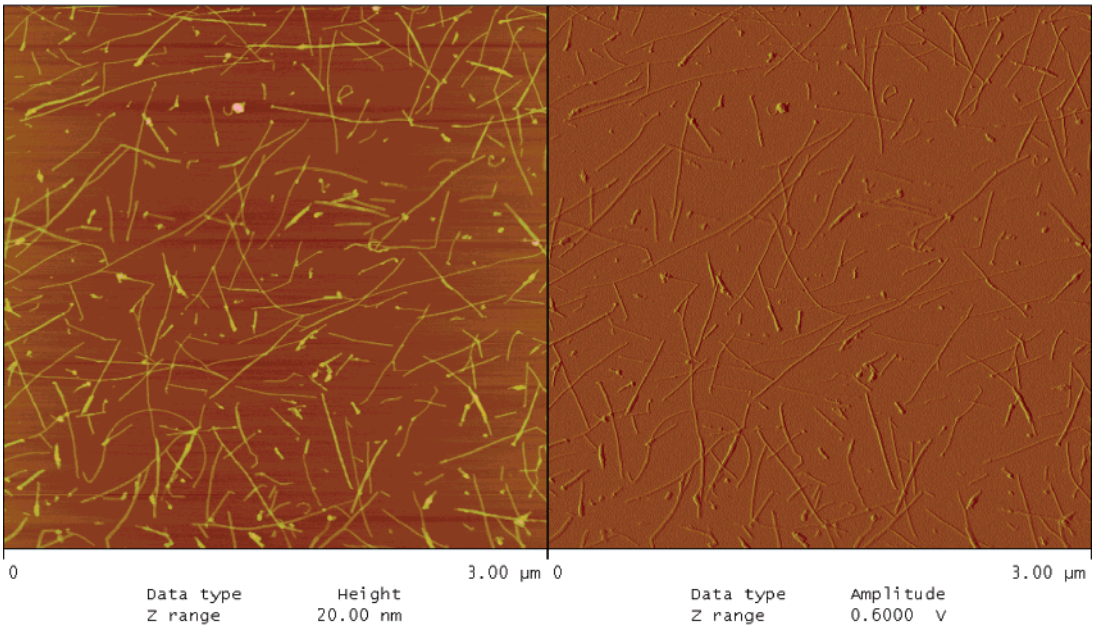

Figure 10. AFM of the nonpolar component from separation method I obtained by spin-coating a DMF solution onto mica.

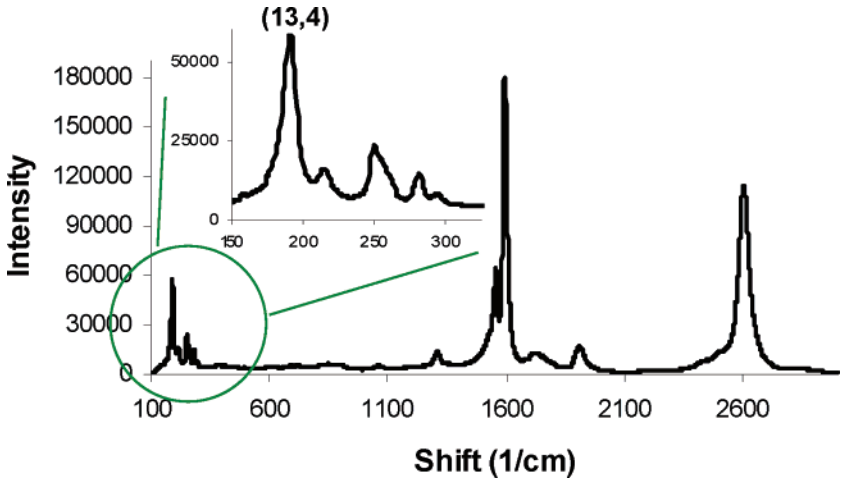

Figure 11. Raman (633 nm excitation) analysis of the nonpolar, regenerated component from separation method I. The inset is the expanded radial breathing mode region.

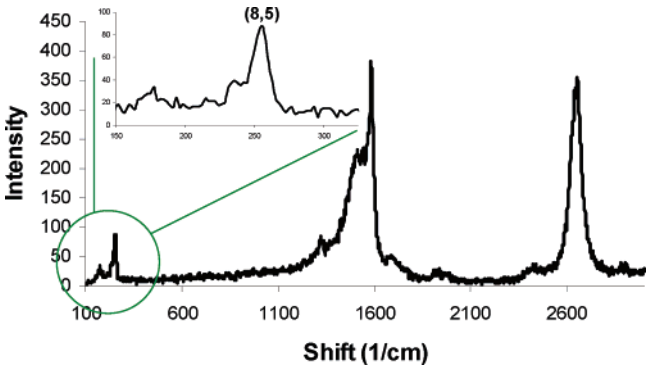

Figure 12. Raman (514.5 nm excitation) analysis of the nonpolar, regenerated component from separation method I. The inset is the expanded radial breathing mode region.

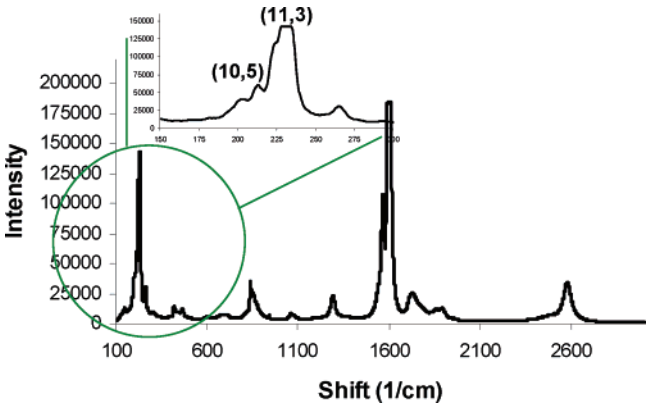

Figure 13. Raman (780 nm excitation) analysis of the nonpolar, regenerated component from separation method I. The inset is the expanded radial breathing mode region.

Anodisc). The supported SWNT mat sample was then dried in vacuo overnight and removed from the membrane as a thin, free-standing nanotube film. The films were mounted on grounded sample holders with tungsten cover shields and loaded into the UHV chamber.

A question that had to be answered was: How many functional groups are appended to the SWNTs after all the van Hove singularities are lost in the absorption spectra? Heavily functionalized material generally has an aryl moiety covalently attached to ca. 1 in 10 SWNT carbons on the nanotube,[16] but selectively functionalized material does

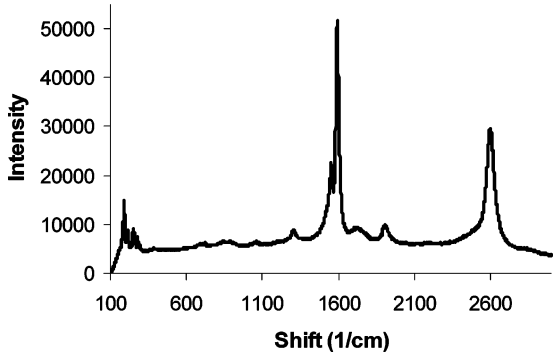

Figure 14. Raman (633 nm excitation) analysis of the polar component from separation method I.

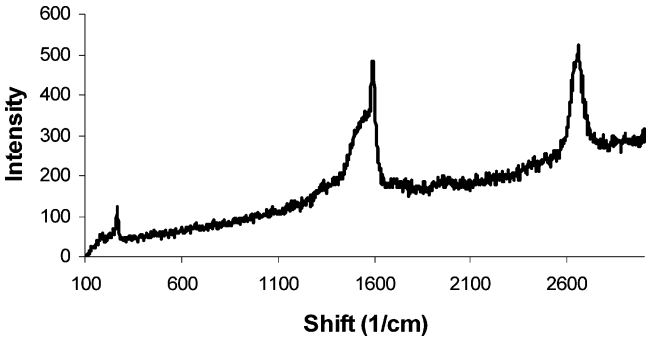

Figure 15. Raman (514.5 nm excitation) analysis of the polar component from separation method I.

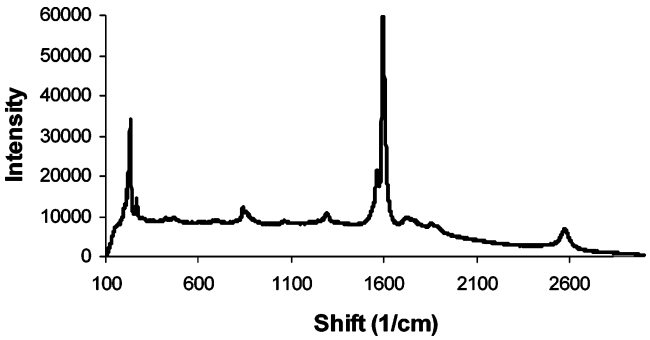

Figure 16. Raman (780 nm excitation) analysis of the polar component from separation method I.

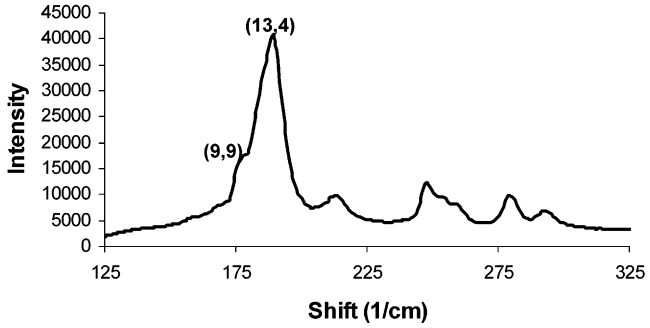

Figure 17. Raman (633 nm excitation) analysis of the nonpolar component enriched in metallics from separation method II.

not have as high a degree of coverage. An estimate of the degree of coverage for selectively functionalized material was determined by functionalizing the SWNTs until all of the van Hove singularities were just lost. This was conducted by reacting the SWNT/SDS solution (100 mL, 0.002 mM, 0.2 mequiv of carbon) with an aqueous solution of 4-fluorobenzenediazonium tetrafluoroborate (3.5 mM) by adding 50

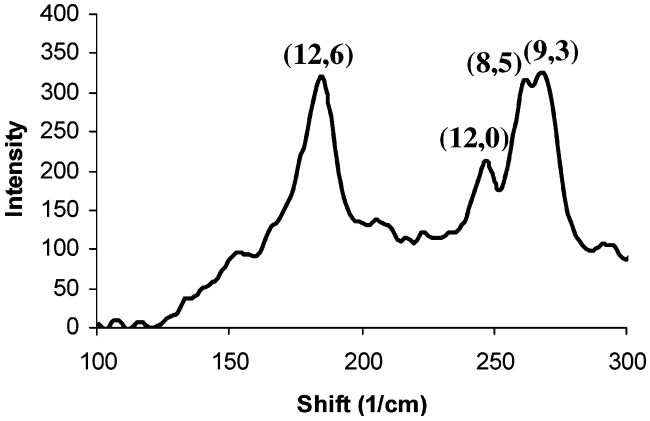

Figure 18. Raman (514.5 nm excitation) analysis of the nonpolar component enriched in metals from separation method II.

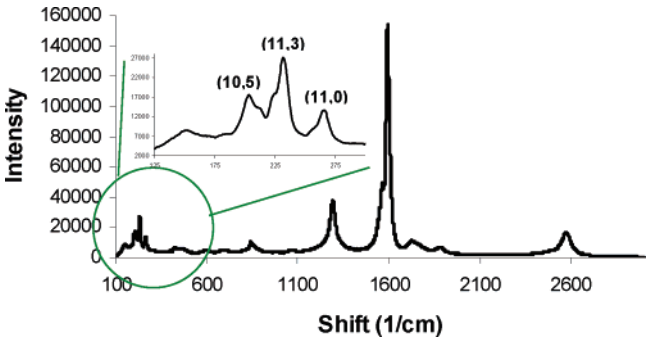

Figure 19. Raman (780 nm excitation) analysis of the nonpolar component from separation method II.

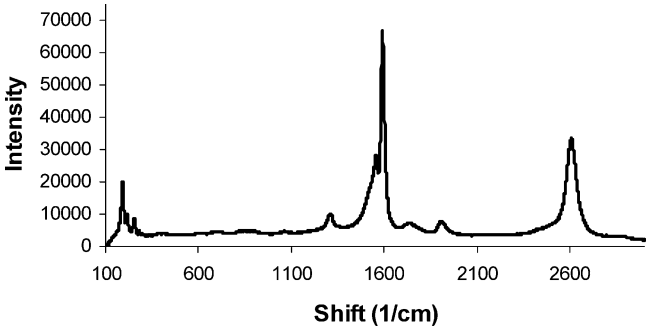

Figure 20. Raman (633 nm excitation) analysis of the polar component from separation method II.

μL every 30 min. The portions were added, and the UV/vis/NIR spectra were monitored after each addition, until all the van Hove singularities (metallics and semiconductors) in the entire spectrum were lost (Scheme 3 and Figure 3). After this, an excess of 4-iodobenzenediazonium tetrafluoroborate (0.254 g, 0.8 mmol) was added (Scheme 3 and Figure 3). The addition of this latter aryl iodide did not affect the UV/vis/NIR spectra, since all the transitions were already lost after addition of the aryl fluoride. The material was treated as described above; it was not filtered through silica gel. After purification of the material by dispersing in DMF with mild sonication, filtering over PTFE and washing with acetone, it was dried in a vacuum oven at 70 °C overnight. The dried, functionalized SWNT was analyzed by XPS to determine the degree of coverage required to lose the optical properties of the nanotube sample. It is apparent from XPS (Figure 4) that the SWNTs react even after the optical properties are lost. The first sample analyzed was mixture **4**, which was reacted until the van Hove singularities were just lost, and the C to F ratio was 99:1. The second sample analyzed was mixture **5**, which had a C to F to I ratio of 93:1:7, therefore, for every 1 fluoride atom on the nanotube there are ca. 7 iodide atoms.

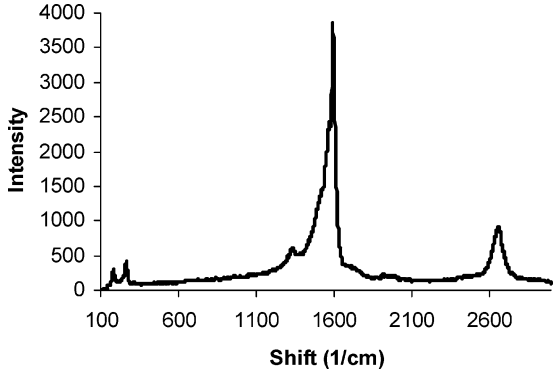

Figure 21. Raman (514.5 nm excitation) of the polar component from separation method II.

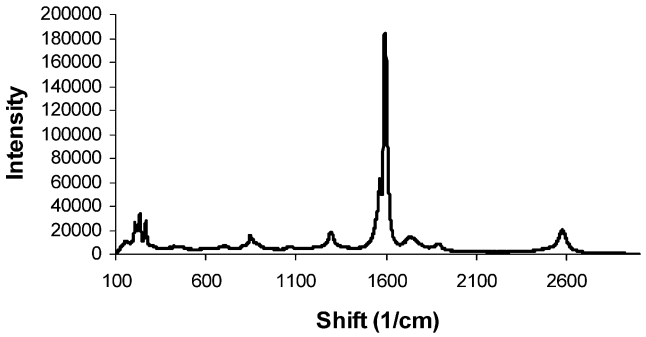

Figure 22. Raman (780 nm excitation) of the polar component from separation method II.

TGA of this same material gave a 7.5 wt % loss for mixture **4** which corresponds to 1 in 100 carbons on the nanotube with an aryl fluoride moiety appended. TGA of the fully functionalized mixture **5** had a 50 wt % loss which corresponds to ca. 1 in 14 carbons on the nanotube bearing an aryl iodide or aryl fluoride moiety. This suggests that approximately only 1 in 100 carbons on the SWNTs are required to react to lose the optical properties.

The appended aryl moieties can be considered defect sites, since, at the reactive site on the nanotube sidewall, an sp^2-C is converted into an sp^3-C. This causes the nanotube to lose resonance at that excitation energy. Therefore, this study also serves as a predictor for the degree of defects on carbon nanotubes. In applications where the electronic or optical properties of SWNTs are required, clearly the fewer defects, the better. At the same time, if the application causes defects, the efficiency will reduce considerably until the optical properties are lost. However, the sidewall chemisorption reaction is reversible upon heating, as seen in Figure 5, which tracks the photoelectron intensity of iodine in a SWNT sample bearing 4-phenyl addends. Upon heating the iodophenyl-grafted nanotube sample above 400 °C, the loss of iodine follows a similar profile as seen in earlier TGA analyses of sidewall reacted SWNT material using diazonium salts (Figure 6).[16,18]

Raman Spectroscopy Background. The Raman spectra were obtained on a Renishaw Ramascope which was equipped with 514.5, 633, and 780 nm lasers. The spectra obtained with the 780 nm excitation were performed with a grating of 1200 l/mm, and the 514.5 and 633 nm employed an 1800 l/mm grating. All of the nanotube samples were purified and dried prior to analysis and the solid samples were mounted on a glass slide with double-sided tape. The experiments were performed with four accumulations each with an exposure time of 10 s to ensure consistency over each irradiated area of the sample. The data were collected and analyzed with Wire 2.0 software.

The resonance Raman enhancement effect for a given nanotube type occurs when the laser excitation wavelength approaches the wavelength of the van Hove singularity of that SWNT. Therefore, any one laser only probes a limited subset of SWNT types. For the purposes of this report, the three excitation wavelengths used to determine the content of the HiPco-derived sample are 514.5, 633, and 780 nm. Figure 1 shows the three wavelengths of excitation used in relation to the van Hove singularities in the absorption spectra. The line at 630 nm divides the spectra where the transitions to the right correspond to only semiconductors and the first three peaks to the left correspond to only metallics. The 514.5 nm excitation probes only metallics and semimetallics (and large diameter semiconductors, but HiPco tubes have few of these, while other sources of SWNTs can show semiconductors at 514.5 nm), the 633 nm excitation probes metallics and semiconductors, and the 780 nm excitation probes only semiconductors. Figure 7 is the assigned radial breathing mode region at 633 nm excitation of the starting SWNT/SDS mixture (prepared for Raman analysis by acetone flocculation, filtration and drying), and Figures 8 and 9 are 514.5 and 780 nm excitations, respectively. The assignment of SWNT chiral vectors (*n* and *m* values) from radial breathing mode frequencies observed in the samples is based on the Strano-revised Kataura plot.[21]

Sample Preparation for Raman Analyses. In cases for the Raman spectra of the starting SWNTs, the materials had been SDS-wrapped, then flocculated from solution with acetone, filtered over PTFE, further acetone-washed to ensure SDS removal, and dried in vacuo. The SWNTs generated from separation methods I and II were used directly from the TGA pan (vide supra). The SWNTs generated from thermolysis of **1** (Scheme 1, prior to filtration through silica gel) were prepared by flocculating the functionalized SWNT/SDS with acetone, filtering over PTFE, washing with acetone, and drying in vacuo and then were thermalized in a TGA apparatus and used directly from the TGA pan.

AFM and Raman Analyses of Eluents from Separation Method I. AFM analysis of the nonpolar fraction (Figure 10) from separation method I (Scheme 1), prior to functional group removal upon thermalization, shows a predominance of individual functionalized SWNTs, with a few bundles and no roped SWNTs, in a broad distribution of lengths. This is analogous to what we observed previously from similar functionalization reactions. Therefore, the sample is not separated by length. Furthermore, while there has been speculation that sonication can cut longer SWNTs, the SWNTs that have been obtained from the Rice University HiPco reactors has predominantly been 100−200 nm in length as determined by AFM on functionalized individual SWNTs that had not undergone sonication.[22] Thus the majority of the SWNTs obtained here seem uncut by the sonication process used. While SWNT length will affect affinity to the stationary phase, the diversity of SWNT lengths that are available to us makes it impossible to assess the overall effect of such polydispersity.

Raman analysis of the component of the heavily functionalized material from separation method I is enriched in the (13,4) and the (8,5) species, which are metallics (Figures 11 and 12, respectively), but it is also enriched in the (11,3) semiconductor (Figure 13). Therefore, enrichment of tube type is indeed apparent in this nonpolar component from separation method I, albeit not exclusive in tube-type segregation.

Raman analysis of the polar fraction from separation method I at 633, 514.5, and 780 nm excitation (Figures 14−16, respectively) showed that the radial breathing mode region is more similar to the spectrum of the starting material than the nonpolar component. The detailed comparison of the radial breathing modes is discussed below.

Raman Analyses of Eluents from Separation Method II. In an effort to improve upon the results from separation method I, the more

(21) Strano, M. S. *J. Am. Chem. Soc.* **2003**, *125*, 16148.
(22) Hudson, J. L.; Casavant, M. J.; Tour, J. M. *J. Am. Chem. Soc.* **2004**, *126*, 11158.

Excitation Wavelength	Raman Spectra of Starting SWNTs	Raman Spectra of SWNTs from Separation Method I, Nonpolar Fraction	Raman Spectra of SWNTs from Separation Method II, Nonpolar Fraction
633 nm	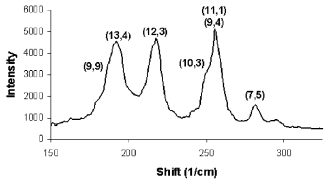 From Fig. 7.	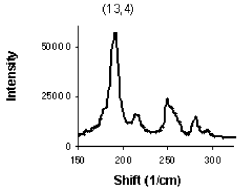 From Fig. 11 inset.	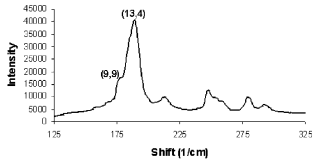 From Fig. 17.
514 nm	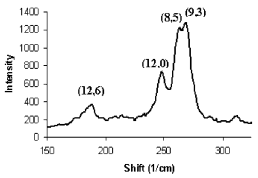 From Fig 8.	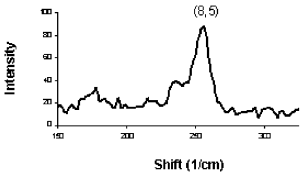 From Fig. 12 inset.	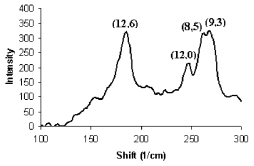 From Fig. 18.
780 nm	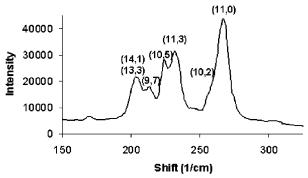 From Fig 9.	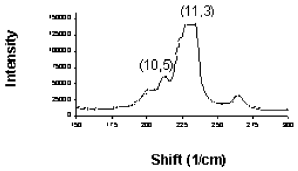 From Fig. 13 inset.	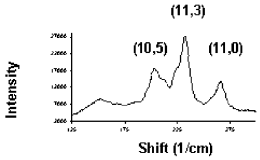 From Fig 19 inset.

Figure 23. Comparison chart of the Raman spectra at varying wavelengths of the starting SWNT (left column, prepared from the SDS/SWNTs by flocculation with acetone), the regenerated (TGA pan) SWNTs from separation method I (middle column), and separation method II (right column).

controlled, but operationally more complex, separation method II (Scheme 2) was conducted. This protocol was devised to allow the polar semiconductors to migrate slower and the nonpolar metals to elute more rapidly from the column with nonpolar solvents as the mobile phase. Both the nonpolar and polar fractions were collected, and the unfunctionalized SWNT structure was regenerated thermally (TGA apparatus) and the two samples were analyzed by Raman spectroscopy (Figures 17−22). The 633 nm excitation (Figure 17) of the nonpolar fraction shows enrichment of the (13,4) metallics. At 514.5 nm (Figure 18), there was significant enrichment in the (12,6) metallic SWNT, along with the three other metallics (12,0), (8,5), and (9,3). By comparing Figure 18 to Figure 12, separation method II significantly favors extraction of the (12,6) SWNT into its nonpolar component. Thus separation method I is more discriminating in tube type as judged by the 514 nm analysis, but complementary to separation method II. Furthermore, the 780 (Figure 19) nm excitation analysis, which probes semiconductors only, shows that there are three semiconductors present in the nonpolar fraction from separation method II, namely (10,5), (11,3), and (11,0), similar to the nonpolar fraction from separation method I. The semiconductors that are probed by this wavelength are much lower in intensity and have a disorder mode (D-band) larger than all other samples, although they were treated by the same thermalization protocol. Thus either these functionalized SWNTs are resistant to defunctionalization or the D-band here does not correspond to the addend sites but to other defects on the sidewall of the nanotubes. Thus, detailed analysis of the breathing modes at 780 nm excitation for separation method II could be complicated due to the large remaining D-band. The polar component that was also analyzed by Raman spectroscopy at three different wavelengths (Figures 20−22) is further discussed below in light of the detailed radial breathing mode comparisons.

A side-by-side comparison of the Raman-active radial breathing modes generated from the starting SWNT/SDS that had been flocculated from acetone and those obtained from separation methods I and II are shown in composite Figure 23. This underscores the observation that both separation methods provide similar enrichment levels when viewing at 633 nm. At 514.5 nm, the operationally simpler separation method I provides a more narrow distribution of SWNT types in favor of the (8,5) metallic, while separation method II affords more of the (12,6) and (9,3) metallics in addition to the (8,5) metallic. Likewise, at 780 nm, separation method I appears more discriminating in favor of the (11,3) semiconductor.

Interpretation of Raman Spectra Affected by Morphology and Excitation Wavelength. Strano and co-workers have recently shown that relative peak intensity changes in Raman spectra can be caused by morphological changes in SWNT bundling.[3,9c] The relative peak intensity changes can therefore result in a misleading impression of separations. Therefore, in an effort to more accurately compare our separation methods I and II samples against compounds regenerated from a TGA apparatus, we took a sample of **1**, heavily functionalized SWNTs prepared according to Scheme 1 but prior to filtration through silica gel, and subjected it to SDS and solvent removal and then addend cleavage at 700 °C, followed by recording of the Raman spectra from the material generated in the TGA pan. The radial breathing modes at 633, 514.5, and 780 nm are shown in Figures 24−26, respectively. Interestingly, when comparing Figures 24−26 with the spectra in Figure 23, column 1, there are noticeable differences that could indeed be morphologically based rather than intrinsic to differing SWNT (*n*,*m*) compositions.

Final composite stacked plots of electronically standardized radial breathing mode data for all of the spectra in this paper are shown in Figures 27−29 at 633, 514.5, and 780 nm excitation wavelengths,

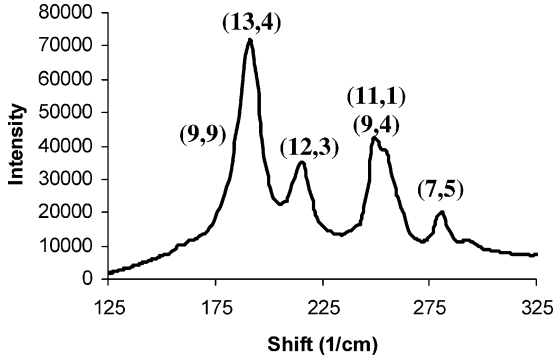

Figure 24. Raman (633 nm excitation) of the radial breathing modes of the SWNTs that had been regenerated (700 °C) from **1** (Scheme 1, after functionalization with 4-*tert*-butylphenyl moieties but prior to filtration through silica gel).

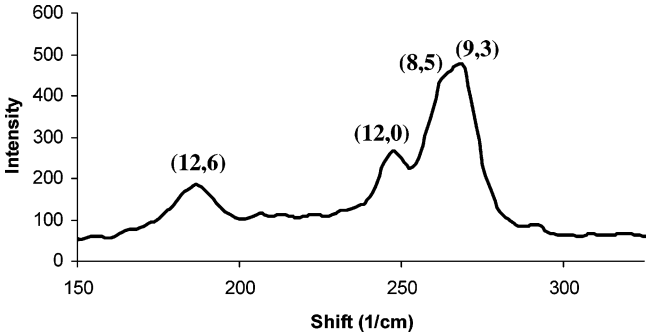

Figure 25. Raman (514.5 nm excitation) of the radial breathing modes of the SWNTs that had been regenerated (700 °C) from **1** (Scheme 1, after functionalization with 4-*tert*-butylphenyl moieties but prior to filtration through silica gel).

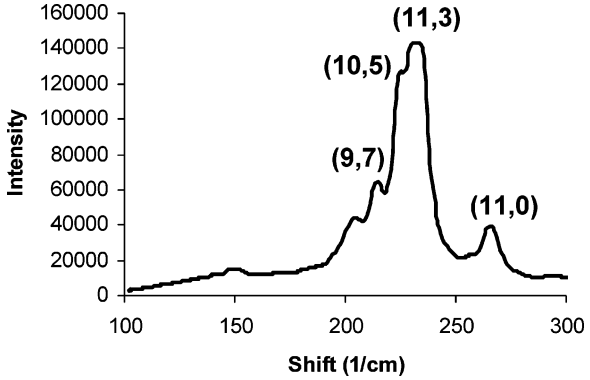

Figure 26. Raman (780 nm excitation) of the radial breathing modes of the SWNTs that had been regenerated (700 °C) from **1** (Scheme 1, after functionalization with 4-*tert*-butylphenyl moieties but prior to filtration through silica gel).

respectively. There were indeed some changes in relative peak heights between the Raman spectra of the functionalized/thermally defunctionalized samples derived from **1** and those of the starting SWNT/SDS samples that had been acetone-flocculated and washed. This difference is apparent at 633 nm (comparing relative intensities in Figures 27a to Figure 27b) and 780 nm (comparing Figure 29a with 29b). For example, at 633 nm (Figure 27a and 27b), signals for the (11,1) and (9,4) are greatly reduced in the thermally treated material. Likewise at 780 nm (Figure 29a and 29b), there is a large suppression of the (11,0) band in the thermally treated SWNTs. Interestingly, the morphological differences are not as noticeable at 514.5 nm (comparing Figure 28a with 28b), thus emphasizing the need to probe the Raman excitations at multiple wavelengths.

At 633 nm (Figure 27), the most noticeable difference is the decline in intensity of the (11,1) and (9,4) semiconductors relative to the

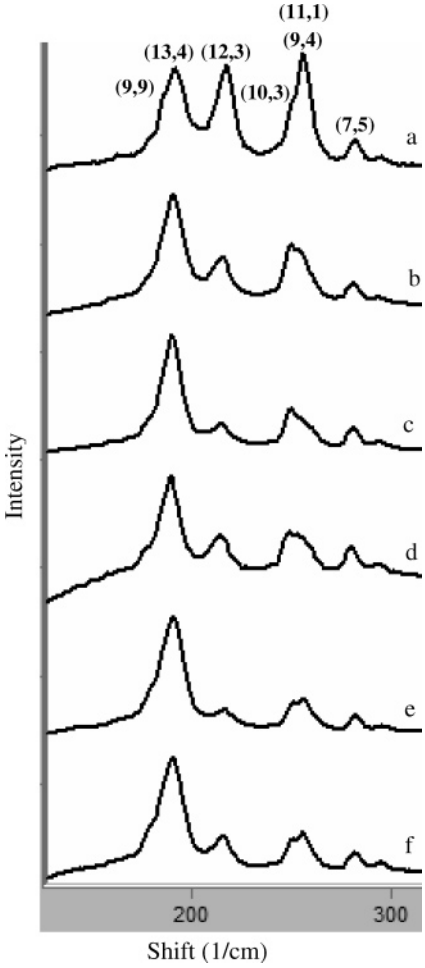

Figure 27. Comparison stacked plots of the Raman (633 nm excitation) spectra of the radial breathing modes of the (a) SWNT/SDS flocculated with acetone, filtered over PTFE, washed with acetone, and dried in vacuo; (b) SWNTs that had been regenerated (700 °C) from **1** in a TGA pan; (c) nonpolar component of separation method I regenerated (700 °C) in a TGA pan; (d) polar component of separation method I regenerated (700 °C) in a TGA pan; (e) nonpolar component of separation method II regenerated (700 °C) in a TGA pan; and (f) polar component of separation method II regenerated (700 °C) in a TGA pan. The peak intensities are in arbitrary units and only relatively comparable within a single trace.

metallics in the sample. Likewise, the polar and nonpolar fractions from both separation methods I and II appeared reasonably similar.

At 514.5 nm (Figure 28), separation method I is clearly superior to separation method II in separating the (12,6) metallic SWNTs from the (8,5) SWNTs. The polar and nonpolar fraction from separation method I are also similar.

At 780 nm (Figure 29), there is a clear difference between separation methods I and II with respect to removal of the (11,0) SWNTs and the segregations between the (10,5) and (11,3) bands.

In total, upon comparing the spectra derived from **1** and the spectra derived from separation methods I and II at multiple excitation wavelengths, the morphological changes alone are not sufficient to account for the relative peak changes noted in our filtration-enriched samples generated here. Indeed, some modest enrichment had occurred in the silica gel-filtration protocols, albeit not as pronounced as one would have been led to believe from a comparison of the flocculated SWNTs to the thermally regenerated SWNTs from separation methods I and II.

Summary and Conclusions

A separation of SWNTs by type was conducted by changing the chemical properties of the metallic SWNTs in relation to

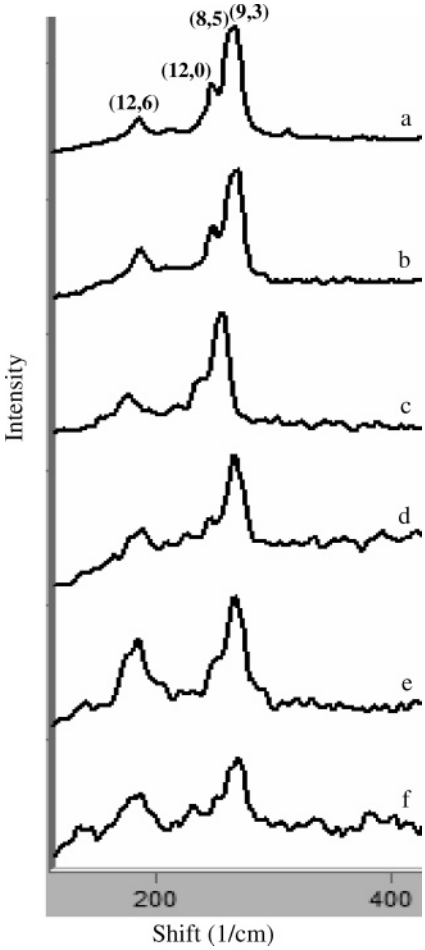

Figure 28. Comparison stacked plots of the Raman (514.5 nm excitation) spectra of the radial breathing modes of the (a) SWNT/SDS flocculated with acetone, filtered over PTFE, washed with acetone, and dried in vacuo; (b) SWNTs that had been regenerated (700 °C) from **1** in a TGA pan; (c) nonpolar component of separation method I regenerated (700 °C) in a TGA pan; (d) polar component of separation method I regenerated (700 °C) in a TGA pan; (e) nonpolar component of separation method II regenerated (700 °C) in a TGA pan; and (f) polar component of separation method II regenerated (700 °C) in a TGA pan. The peak intensities are in arbitrary units and only relatively comparable within a single trace.

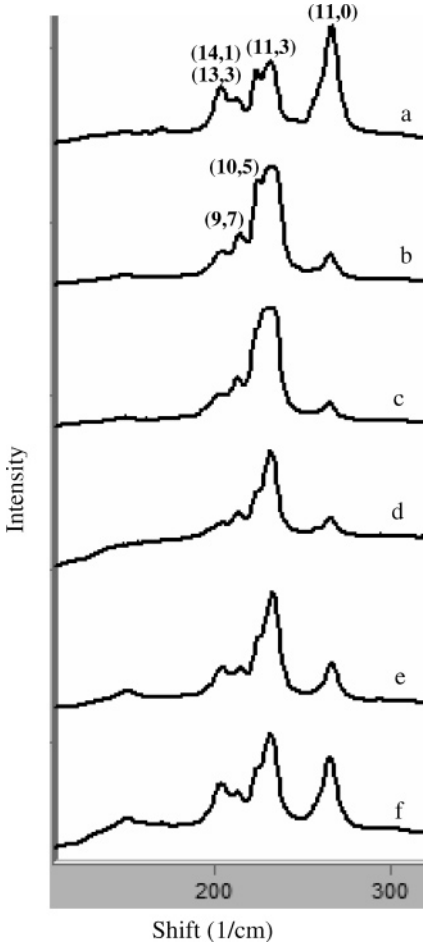

Figure 29. Comparison stacked plots of the Raman (780 nm excitation) spectra of the radial breathing modes of the (a) SWNT/SDS flocculated with acetone, filtered over PTFE, washed with acetone, and dried in vacuo; (b) SWNTs that had been regenerated (700 °C) from **1** in a TGA pan; (c) nonpolar component of separation method I regenerated (700 °C) in a TGA pan; (d) polar component of separation method I regenerated (700 °C) in a TGA pan; (e) nonpolar component of separation method II regenerated (700 °C) in a TGA pan; and (f) polar component of separation method II regenerated (700 °C) in a TGA pan. The peak intensities are in arbitrary units and only relatively comparable within a single trace.

the semiconductor SWNTs and then performing filtration through silica gel. The nonpolar component from separation methods I and II were enriched in the metallic nanotubes. Separation method I was operationally simpler and complementary to separation method II for certain tube-type segregations, especially when probed at 780 nm. We can rationalize the functionalized metallics being less polar than the functionalized semiconductors in separation method II because the semiconductors had hydroxylated addends. However, what was the segregation mode between metallics and semiconductors in separation method I wherein the 4-*tert*-butylphenyl addend was the only functionality used? We can speculate that some metallic SWNTs were more heavily functionalized than the semiconductors in separation method I, therefore making them less polar and more prone to migration on silica gel. Use of less disperse SWNT starting materials or use of HPLC on silica gel would likely afford greater separation efficacies on the functionalized SWNTs. The pore size of the silica gel is 150 Å, thus the pore size is likely too small for significant size-exclusion-based length discrimination of these rigid structures.

A careful comparison was made between the Raman spectra of the silica gel filtration-enriched samples and those of SWNTs of varying morphologies prepared from flocculation or thermal regeneration.[3] If comparison had been made from only the flocculated material derived from the SWNT/SDS material, a false impression for enrichment efficacy would have been made. The analyses underscored the need to compare similar deposition methods and multiple excitation wavelength Raman analyses. And finally, the study here provided a correlation between the van Hove singularities in the UV/vis NIR spectra and the degree of functionalization as assessed by XPS.

Acknowledgment. We thank NASA, ONR, AFOSR, NSF, and DARPA for their gracious support of our SWNT research program and Professor Richard E. Smalley for the supply of HiPco SWNTs via the Carbon Nanotechnologies Laboratory at Rice University.

JA042828H